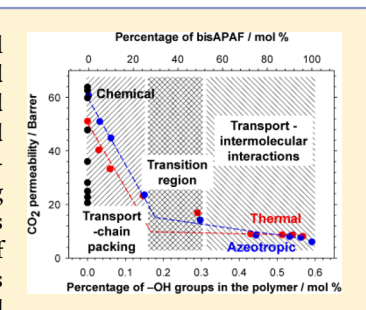


Influence of the Composition and Imidization Route on the Chain Packing and Gas Separation Properties of Fluorinated Copolyimides

Alberto Tena,*^{,†} Sergey Shishatskiy,[†] David Meis,[†] Jan Wind,[†] Volkan Filiz,[†] and Volker Abetz^{†,‡}

ABSTRACT: A strong effect of the chemical composition and imidization method on physical and especially on gas transport properties of polyimides was demonstrated. Two fluorinated diamines 6FpDA and bisAPAF were polymerized in different ratios, employing the fluorinated dianhydride 6FpDA to get polyimides with nine different compositions. For all synthesized materials three imidization methods were used: azeotropic, thermal, and chemical. The 6FpDA-6FpDA homopolymers showed significant differences in the gas transport properties, indicating the influence of the imidization route on the final properties of the polyimides. For polyimides containing bisAPAF, the chemical composition played an important role due to the exchange of the hydroxyl groups by acetate groups leading to different interchain interactions. The gas transport was mainly controlled by the chain packing for thermally and azeotropically imidized



polymers with bisAPAF contents lower than 30 mol %. For bisAPAF contents above 50 mol % the gas transport was controlled by the intermolecular interactions, e.g., hydrogen bonds.

■ INTRODUCTION

The term "high-performance material" is usually applied to the material, which has one or, even better, a number of properties close to or exceeding the maximum value known up to date. Aromatic polyimides with high thermal resistance, low density, high mechanical strength, high conductivity, high thermal, and superior flame resistance ^{1,2} properties, which allow their use for advanced biomedical and engineering applications including various separation processes, are often referenced to as high-performance polymers. ^{3–6}

Fully aromatic polyimides have high chain rigidity and strong intra- and interchain interactions due to the charge transfer complex (CTC) formation and electronic polarization. This leads to a poor processability as a consequence of low solubility, which results in applicability limitations. Therefore, the processing of polyimides is usually carried out using soluble poly(amic acid) precursors. However, the process has inherent limitations, including storage instability of the poly(amic acid) intermediate. The conversion of the poly(amic acid) into polyimide is done through the imidization reaction step which can be performed by three different routes: azeotropic, thermal, or chemical imidization set. The insolubility of the final polyimide, however, limits the choice of imidization method for aromatic polyimides after membrane casting, especially in the case of the thermal imidization. 13,14

Improvement of polyimides solubility had been studied using several approaches, generally related to the reduction of the backbone rigidity, chain packing, and/or CTC interactions by disruption of the polymer chain linearity by introducing flexible linkages, bulky substituents, and noncoplanar or alicyclic monomers. Among these approaches, the presence of fluorine in polyimides improves the solubility, reduces the dielectric constant, water absorption, and even color, and

improves optical transparency, ²⁶ thermal resistance, ²⁷ or fractional free volume. ^{28,29}

The fractional free volume has a direct influence on the transport of small molecules in polymeric materials.³⁰ In this sense, several studies have evaluated the relation between presence of fluorine-containing structures and separation properties of polymers.^{30–32} In the case of fluorinated polyimides, one of the most studied monomers is the 4,4′-(hexafluoroisopropylidene)diphthalic dianhydride (6FDA). Its presence in the polyimide leads to relatively high permeabilities and permselectivities combined with good mechanical, chemical, and thermal properties.^{33–43}

Surprisingly, the influence of the imidization route of poly(amic acid)s conversion to polyimides on gas transport properties has not been sufficiently considered, most probably due to the assumption that imidization leads to the same or mostly the same structure of the polyimide and thus cannot influence the gas transport properties significantly. Only one work, presented by Han et al., has pointed to a significant impact of the imidization route on physical and gas transport properties of thermally rearranged (TR) polymers and its effect on the physical properties of polyimides derived from 6FDA and the diamine 2,2-bis(3-amino-4-hydroxyphenyl)hexafluoro-propane (bisAPAF).⁴⁴

Here, we prepared and characterized polyimides derived from the reaction between the dianhydride 6FDA and the diamine 2,2-bis(4-aminophenyl)hexafluoropropane (6FpDA) and from the reaction between 6FDA and bisAPAF as well as the copolymers derived from the combination between the

Received: May 21, 2017 **Revised:** July 13, 2017

[†]Institute of Polymer Research, Helmholtz-Zentrum Geesthacht, Max-Planck-Str. 1, 21502 Geesthacht, Germany

[‡]Institute of Physical Chemistry, University of Hamburg, Martin-Luther-King-Platz 6, 20146 Hamburg, Germany

Figure 1. Structure of the copolymers synthesized in this work. R = -H for copolymers obtained by azeotropic (Az) and thermal (T) imidization, and R = -AcO for copolymers obtained by chemical (Ch) imidization; x + y = 100, and values for the mol % content of bisAPAF "y" in the structure are 0, 5, 10, 25, 50, 75, 90, 95, or 100.

dianhydride 6FDA and the diamines 6FpDA and bisAPAF in seven different mol % of 6FpDA:bisAPAF (95:5; 90:10; 75:25; 50:50; 25:75; 10:90, and 5:95). The poly(amic acid) precursors were prepared in the same way for all the studied materials, and afterward, three different imidization methods were employed: azeotropic (Az) imidization, which uses a solvent that forms an azeotrope with H2O (such as xylene), which is afterward evaporated from the mixture; thermal (T) imidization, which induces exothermic ring closure by dehydration during thermal treatment at high temperatures; and chemical (Ch) imidization, which is performed by the chemical reaction of acetic anhydride with the poly(amic acid) under basic conditions. The effects of imidization routes, polymer composition, and polymer chain interactions on the chemical structure as well as physical and gas transport properties of the synthesized polyimides were studied.

■ EXPERIMENTAL SECTION

Chemicals. 4,4'-(Hexafluoroisopropylidene)diphthalic anhydride (6FDA), 2,2-bis(4-aminophenyl)hexafluoropropane (6FpDA), and 2,2'-bis(3-amino-4-hydroxylphenyl)hexafluoropropane (bisAPAF) were purchased from Sigma-Aldrich. 6FDA was purified by sublimation at high vacuum just before use. Diamines were dried at 120 °C under vacuum for 12 h and stored in an evacuated desiccator until use.

Reactants and solvents, such as chlorotrimethylsilane (CTMS), pyridine (Py), acetic anhydride, N,N-dimethylaminopyridine (DMAP), o-xylene, and anhydrous N-methyl-2-pyrrolidinone (NMP) of reagent-grade quality were all purchased from Sigma-Aldrich and were used without further purification.

Poly(amic acid) Synthesis. A set of 27 copolymers were synthesized in this work. For all copolymers the first part of the reaction was the formation of the corresponding poly(amic acid), and the same synthesis route was followed. The polyimides were synthesized following the classical in situ silylation two steps method.³⁵ A three-necked flask, equipped with a mechanical stirrer and gas inlet and outlet, was charged with 5.0 mmol of the corresponding mixture of diamines 6FpDA (x) and bisAPAF (y) and 5.0 mL of solvent (NMP). The solution was stirred at room temperature under an argon atmosphere until the solid was completely dissolved. Then, the solution was cooled, by the use of an ice bath, to 0 °C, and the required amount of CTMS and pyridine (1 mol/mol reactive group) and small amounts of DMAP (0.1 mol/mol pyridine) were added to the mixture. At that moment, the temperature was raised up to room temperature to ensure the formation of the silylated diamine. After this, the corresponding dianhydride 6FDA (5.0 mmol) and additional solvent were added. The reaction mixture was left overnight to ensure the formation of the corresponding poly(amic acid) in the solution. The viscosity of the solution significantly increased during this period.

Various copolymer compositions were synthesized, where mol 6FpDA (x) + mol BisAPAF (y) = 100, and the values of y were 0, 5, 10, 25, 50, 75, and 100 in mol %. Figure 1 shows the structure of the copolymers synthesized in this work. Composition of the copolymers and nomenclature used in this work are shown in Table 1.

Imidization Methods. Three different methods were employed to carry out the imidization of the poly(amic acid) in order to obtain the corresponding polyimide. Azeotropic and chemical imidization were

Table 1. Properties of the Copolymers Obtained with Different Imidization Methods and BisAPAF Content

imidization method	bisAPAF content (mol %)	acronym	$M_{\rm w} \ ({ m kg\ mol}^{-1})$	PDI	$({}^{\circ}\overset{T}{C})$
azeotropic	0	0% Az	280	2.1	308
	5	5% Az	170	1.8	305
	10	10% Az	345	1.8	306
	25	25% Az	96	4.0	304
	50	50% Az	204	5.7	301
	75	75% Az	56	2.3	304
	90	90% Az	160	5.9	303
	95	95% Az	155	5.6	300
	100	100% Az	111	3.6	304
thermal	0	0% T	65	3.0	311
	5	5% T	205	2.7	308
	10	10% T	165	6.0	305
	25	25% T	179	4.2	307
	50	50% T	158	4.5	303
	75	75% T	229	2.0	303
	90	90% T	181	2.9	305
	95	95% T	106	2.3	305
	100	100% T	46	1.9	303
chemical	0	0% Ch	90	6.9	310
	5	5% Ch	360	3.0	305
	10	10% Ch	482	2.4	301
	25	25% Ch	260	2.2	291
	50	50% Ch	253	2.0	282
	75	75% Ch	217	1.2	272
	90	90% Ch	82	2.4	263
	95	95% Ch	66	2.5	261
	100	100% Ch	220	3.5	259

applied in the polymer solutions while thermal imidization was carried out in the polymer films.

Azeotropic Imidization. o-Xylene (10 mL) was added as an azeotropic agent to the poly(amic acid) solution, which was stirred vigorously and kept heating to 180 °C for 6 h to promote imidization. During this period, the water released by the ring-closure reaction, silanol, and siloxane byproducts were separated as a xylene azeotrope. Thereafter, leftover o-xylene was distilled from the polymer solution, the mixture was cooled to room temperature, and finally the polymer was precipitated in distilled water. The pristine polymer thus obtained was repeatedly washed in a mixture of water and ethanol and dried under vacuum at 120 °C for 24 h.

Thermal Imidization. Poly(amic acid)s were precipitated in distilled water and repeatedly washed in a mixture of water and ethanol in order to eliminate the solvent and residue of the byproducts from the reaction. Afterward, polymers were dried under vacuum at 120 °C for 24 h. Subsequently, a polymer film was casted from a 10% wt THF solution onto a leveled glass plate at 30 °C. THF was slowly evaporated, and the polymer was removed from the glass. The transparent poly(amic acid) films were placed in a vacuum oven, and the temperature was progressively raised up to 200 °C and left for 24 h to complete the thermal imidization.

Chemical Imidization. An excess of acetic anhydride (20.0 mmol) and pyridine (10.0 mmol) was added to the poly(amic acid) solutions; the obtained mixture was heated to 60 $^{\circ}\mathrm{C}$ and stirred vigorously for 8 h. Afterward, the mixture was precipitated in distilled water and repeatedly washed in a water/ethanol mixture. Polymers were dried under vacuum at 120 $^{\circ}\mathrm{C}$ for 24 h.

Polymer Film Formation. The casting of copolyimide films with uniform thickness was done from a 10 wt % filtered solution in THF as solvent onto a leveled glass plate at 30 $^{\circ}$ C. After slow evaporation of the solvent and formation of a solid film, the formed isotropic polymer films were removed from the glass surface and placed in a vacuum oven equipped with a turbomolecular pumping unit where they were dried for 6 h at 200 $^{\circ}$ C. The defect-free and optically clean membranes were used for the characterization of the materials. TGA study did not reveal any solvent presence in the dry polymer films.

Characterization of the Polymers. ¹H NMR study was accomplished with the Avance 500 spectrometer (Bruker GmbH, Germany) equipped with a 500 MHz magnet and a triple resonance inverse (TXI) probe. The experiments were done at room temperature with deuterated DMSO as solvent and tetramethylsilane as internal standard. Materials were completely soluble in DMSO, and NMR study has confirmed the structure of the imidized polyimides.

Attenuated total internal reflectance—Fourier transform infrared spectroscopy (ATR-FTIR) experiments were conducted in order to verify the imidization of the polymers. ATR-FTIR was performed at room temperature using a Bruker ALPHA FT-IR spectrometer in a spectral range of 400–4000 cm⁻¹ with a resolution of 2 cm⁻¹ and average of 32 scans. Thick membranes were directly measured, and imidization of the copolymers synthesized in the work was confirmed.

Molecular weight of the copolymers was determined by using gel permeation chromatography (GPC) after calibration with polystyrene standards. GPC measurements were performed at 40 °C having DMAc as eluent on a Waters instrument (Waters GmbH, Eschborn, Germany) equipped with polystyrene gel columns of different pore sizes, using a refractive index (RI) detector.

Differential scanning calorimetry (DSC) analysis was used in order to determine the $T_{\rm g}$ of polymers. DSC experiments were done with a calorimeter DSC 1 (Mettler Toledo), within the temperature measurement range from 100 up to 350 °C at a heating rate of 10 K/min for samples azeotropic and thermally imidized and from 100 up to 300 °C at a heating rate of 10 K/min for the samples chemically imidized. Measurements were conducted under a nitrogen atmosphere to prevent oxidation. The glass transitions were determined in the second heating cycle in order to avoid the possible effect of the remaining solvent or other sample preparation history. In our case, first heating cycle was from room temperature up to 250 °C at a heating rate of 10 K/min. One of the monomers used for the synthesis of these copolymers, the diamine bisAPAF, in combination with the dianhydride 6FDA, has the possibility to undergo to benzoxazole by thermal rearrangement due to hydroxyl group in the ortho position to the imide group. 45 For this reason, the temperatures used in order to avoid the thermal rearrangement process that could start at temperatures up to 300 °C were temperatures close to the T_{α} of the polymers.

Thermogravimetric analysis (TGA) was used to determine the thermal stability of the copolymers. TGA experiments were carried out on a Thermal Analysis NETZSCH TG209 F1 Iris instrument. The experiments were done in a temperature range from 25 up to 800 $^{\circ}\mathrm{C}$ and at heating rate of 5 K/min under a flux of 20 mL/min of argon. Disc-shaped samples, cut from cast films, with weights between 5 and 15 mg were tested.

Fractional free volume (FFV) was determined from density measurements. A density determination kit (Mettler Toledo, Greifensee, Switzerland) was employed. The auxiliary liquid for the measurement was isooctane. FFV was calculated according to the method described elsewhere. 46

The permeability (P) was determined using a permeator utilizing the "constant volume, variable pressure" approach (known also as time-lag method). ⁴⁷ The permeability coefficient measurements were carried out at 1000 mbar feed pressure and 30 °C for H_2 , H_2 , CH_4 , N_2 ,

 O_2 , and CO_2 . A sketch of the facility and the analysis method used has been described elsewhere.⁴⁸ Permeability values (*P*) were determined according to eq 1:

$$P = \frac{Vl}{At(P_{\rm f} - P_{\rm p})} \tag{1}$$

where V is the permeate system volume (cm³), l is the film thickness (cm), A is the effective film area (cm²), t is the time (s), $P_{\rm f}$ is the feed pressure, and $P_{\rm p}$ is the permeate pressure. The unit of permeability P is barrer, which is 10^{-10} cm³ (STP) cm/(cm² s cmHg). The diffusion coefficients (D) were estimated from time-lag data (θ), according to eq 2:

$$D = \frac{l^2}{6\theta} \tag{2}$$

where θ is the diffusion time lag. Once P and D were calculated, the apparent solubility coefficients (S) were evaluated by following expression:

$$S = \frac{P}{D} \tag{3}$$

From these equations, the ideal selectivity $\alpha_{a/b}$ can be calculated as the ratio of permeability coefficients for the pure gases a and b:

$$\alpha_{a/b} = \frac{P_a}{P_b} \tag{4}$$

By substituting eq 2 in eq 4, the ideal selectivity can be split into two parts:

$$\alpha_{a/b} = \frac{D_a S_a}{D_b S_b} = \alpha_D \alpha_S \tag{5}$$

where $\alpha_{\rm D}$ is the diffusivity selectivity and $\alpha_{\rm S}$ is the solubility selectivity.

■ RESULTS AND DISCUSSION

Three different methods of imidization were employed in this work: azeotropic (Az), thermal (T), and chemical (Ch). In order to simplify the names of the samples, sample labeling was done employing the value of bis-APAF fraction y and by the imidization method. As an example, the polymer imidized by the azeotropic method and with a value of y equal to 25 (which means ratio between diamines 6FpDA (x) and bisAPAF (y) in the copolymer is 75:25 mol %) is named 25% Az. All the acronyms and some properties of prepared samples are collected in Table 1.

The ¹H NMR study has confirmed the success of the imidization procedure and final structures of synthesized polymers. Figure 2 shows the ¹H NMR spectra for the homopolymers, in this case 6FDA-6FpDA, for values of *y* equal to 0, and 6FDA-BisAPAF, for values of *y* equal to 100.

The structures of the homopolymers were completely identified. Apparently, no differences were observed in the case of the 6FDA-6FpDA homopolymers imidized by the three different methods. In the case of the 6FDA-BisAPAF homopolymers, azeotropic and thermal imidization showed comparable spectra; however, chemical imidization, due the synthetic procedure, showed a different spectrum. The existence of the acetate group, as follows from the peak at around 2.1 ppm, and a very small appearance of the –OH group (10.4 ppm) indicated that the functionalization of the hydroxyl group was almost complete. In any case, peaks typical for poly(amic acid) were not obtained, indicating that the imidization was complete. Obviously, in the copolymers' spectra appeared peaks characteristic for both homopolymers, 6FDA-6FpDA and 6FDA-BisAPAF, where the peak's intensity

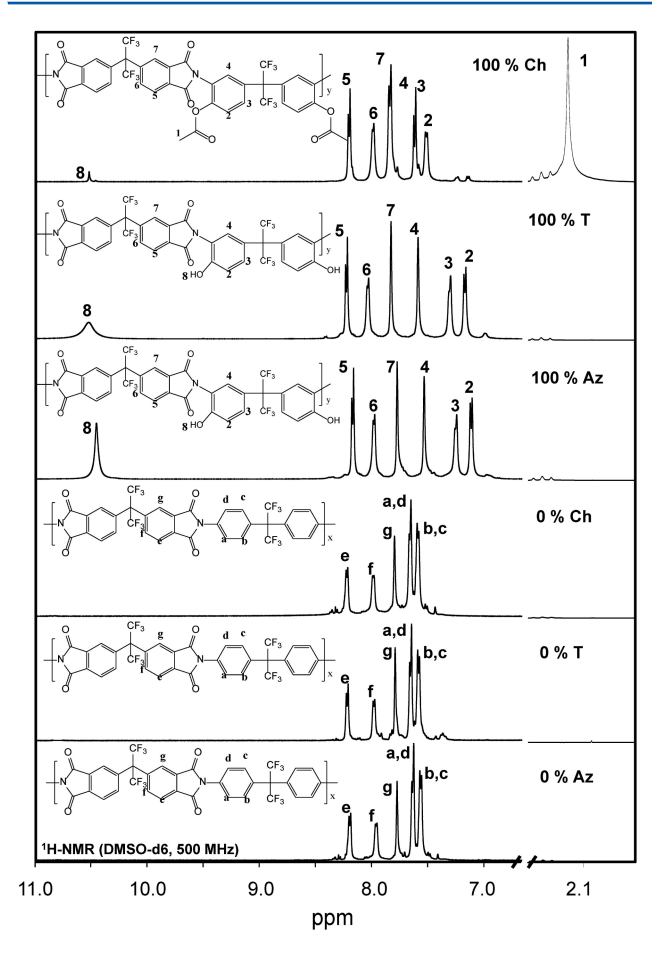


Figure 2. ¹H NMR in DMSO for the homopolymers synthesized by different imidization methods.

is a function of the amount of each component in the final structure. This statement is supported by the ¹H NMR spectra for homopolymers and copolymers synthesized by azeotropic imidization shown in Figure 3.

The obvious evolution from the pure homopolymer 6FDA-6FpDA, when *y* is equal to 0, to the corresponding 6FDA-BisAPAF, when *y* is equal to 100, can be observed from the Figure 3. In all the cases, peaks for the poly(amic acid) were not observed in imidized polymers. Similar behavior was found for the copolymers imidized by thermal and chemical methods.

Chemical structures and completion of imidization processes were revealed by means of FT-IR. 49,50 Figure 4 shows the IR spectra for the homopolymers and copolymers imidized by thermal treatment. Since the structure of the homopolymers is similar in terms of characteristic vibrational bands, differences between imidization methods were not observed, and only small differences in composition were detected. For all the copolymers, complete cyclization was evident from the lack of amide. Figure 4a shows the FT-IR for the homopolymers obtained by different imidization methods. For 6FDA-6FpDA homopolymers where y = 0, symmetric C=O (1782 cm⁻¹), asymmetric C=O (1714 cm⁻¹), C-N stretching (1364 cm⁻¹), and imide ring deformation (714 cm⁻¹) peaks were detected. In the case of the 6FDA-BisAPAF homopolymers where y = 100, small shifts of the peaks were observed: symmetric C=O (100% Az 1789 cm⁻¹, 100% T and 100% Ch 1797 cm⁻¹), asymmetric C=O (100% Az 1730 cm⁻¹, 100% T and 100% Ch 1722 cm⁻¹), C-N stretching (100% Az 1373 cm⁻¹, 100% T

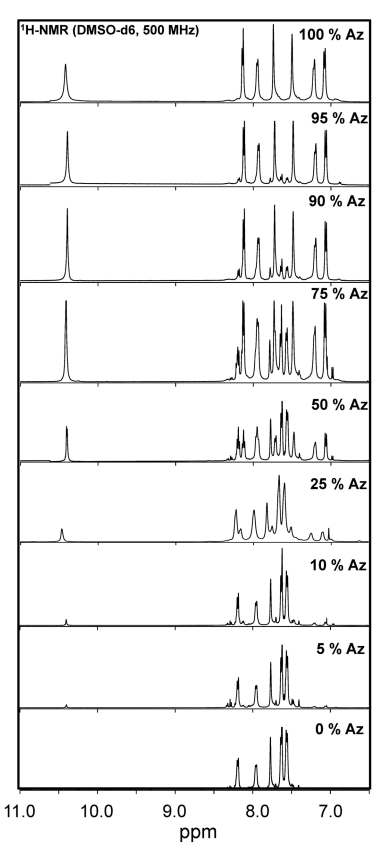
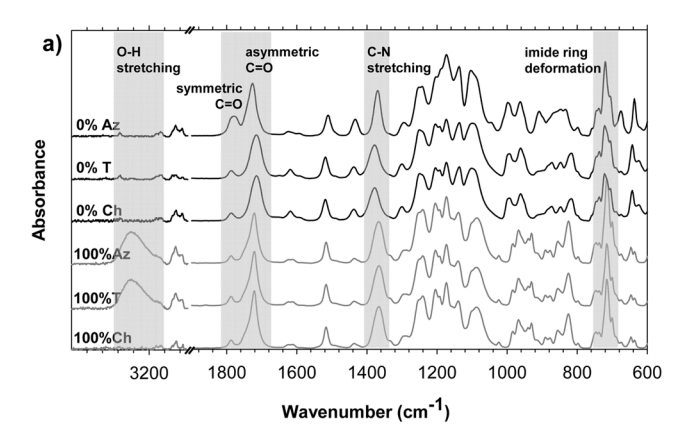


Figure 3. ¹H NMR for homopolymers and copolymers synthesized by azeotropic imidization.

and 100% Ch 1385 cm⁻¹), and imide ring deformation (100% T 724 cm⁻¹, 100Az and 100% Ch 722 cm⁻¹); it appears, as a difference with the 6FDA-6FpDA homopolymers, a broad absorbance corresponding to the hydroxyl group stretching (100% Az 3400 cm⁻¹, 100% T 3400 cm⁻¹ and 100% Ch no detected). Figure 4b shows the FTIR for the set of polymers thermally imidized, where despite the changes being small, it was possible to estimate the evolution between 0% T and 100% T. Apparently, differences in the spectra were not observed for different imidization methods.

As expected, the glass transition temperatures appeared in two different manners (Table 1). Polyimides derived by azeotropic and thermal imidization methods showed very similar values, including a slight decrease of the $T_{\rm g}$ for low bisAPAF content, until 10 mol %, and afterward, keeping almost constant for the rest of the content range. T_g values for the homopolymers were very close to each other, which obviously does not incite significant differences in the T_g values for the copolymers. For polymers derived by chemical imidization a gradual decrease of the $T_{\rm g}$ was found with increase of bisAPAF content in the copolymer. The acetate group attached to the oxygen in the ortho-position to the imide group restricted the possibility of hydrogen bonding and reduced as well the possibility of CTC interactions between the polymer chains. 51,52 Therefore, increasing the amount of acetate groups in the copolymer will reduce the $T_{\rm g}$ in a linear decrease. Referring to the molecular weight of the polymers, no clear tendency was found, despite that a decrease can be expected in the molecular weight when the amount of the bisAPAF is higher in the polymer due to the lower reactivity of this monomer compared to the 6FpDA. Differences in the



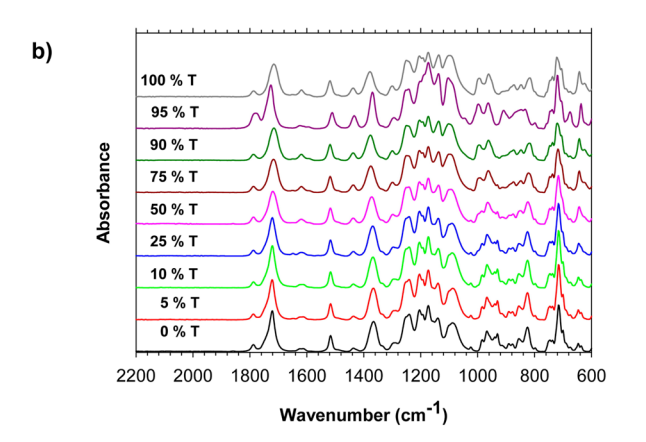


Figure 4. (a) FTIR for the homopolymers obtained by different imidization methods. (b) FTIR for the homopolymers and copolymers imidized by thermal treatment.

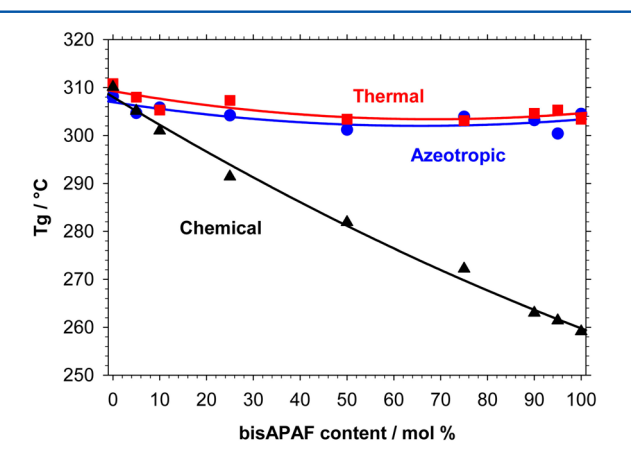


Figure 5. Evolution of the $T_{\rm g}$ as a function of the composition and imidization method for all the materials studied in this work.

molecular weight for the different imidization routes were not clear. 53,54

Thermal stability of the polymers was evaluated by TGA. For all studied samples no weight loss was observed until the temperatures where thermal degradation or thermal rearrangement of the polymers started. No difference in thermal stability was observed as well for samples imidized by three different methods. The homopolyimide 6FDA-bisAPAF has the possibility of undergoing to polybenzoxazole (PBO) structure by thermal rearrangement at temperatures between 350 and 450 °C, with the corresponding weight loss associated with the elimination of carbon dioxide during the rearrangement

process. The weight loss is strongly dependent on the imidization method.⁴⁴ For the homopolymer 6FDA-BisAPAF imidized by azeotropic or thermal methods the weight loss associated with the rearrangement is 11.4%, while the weight loss for the 6FDA-bisAPAF homopolymer, imidized by the chemical imidization method, is 20.25% with respect to the thermal rearrangement (Figure 6). First, this is attributed to the

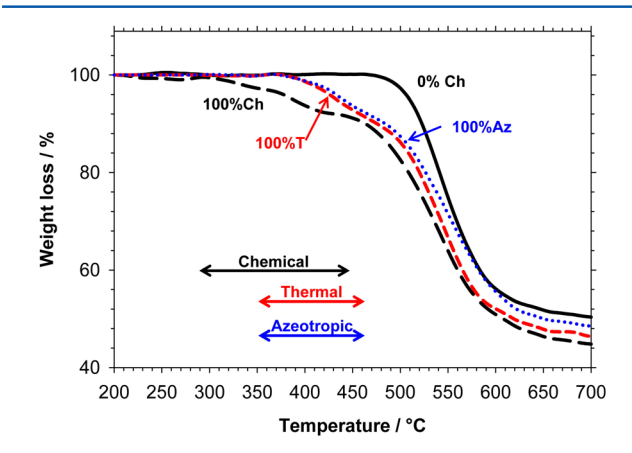


Figure 6. Thermogravimetric analysis for some selected homopolymers.

loss of the acetate group, bonded to the oxygen in the *ortho*-position to the imide group, and later, with the elimination of carbon dioxide during the rearrangement to PBO as it can be seen in Figure 6. Obviously the copolymers will have a weight

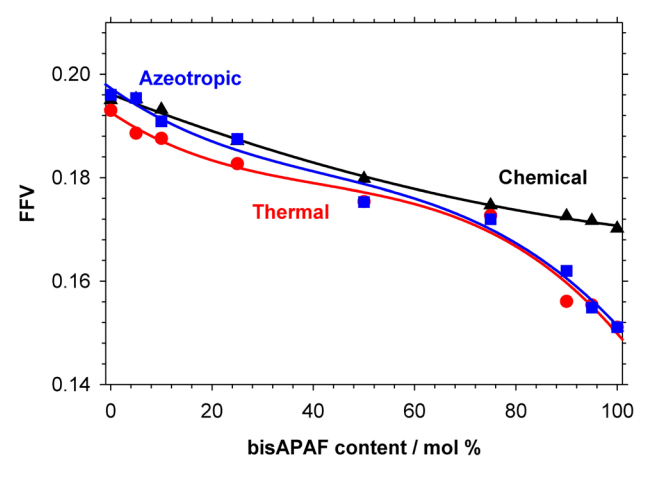


Figure 7. FFV of the samples synthesized in this work calculated by the Bondi group contribution method.

loss related to the imidization process and composition. It is also important to point out that rearrangement process is overlapped by polymer chain degradation process, which normally starts at temperatures above 400 °C for these polymers. Nevertheless, this work focuses on the study of the influence of the imidization method on the properties of polyimides, which are thermally stable until 350 °C, for the polymers derived from azeotropic and thermal imidization, and until 250 °C, for copolymers obtained by chemical imidization method. The rearrangement process will be explained in detail in the future.

Two different approaches were used for the calculation of the theoretical fractional free volume (FFV) of the studied

Table 2. Permeability Coefficients of Pure Gases (30 °C and Feed Pressure 1000 mbar) Compared to the Density and FFV for Polymers under Study

			permeability (barrer)					
sample	density (g cm ⁻³)	FFV	H ₂	He	O ₂	N ₂	CH ₄	CO ₂
0% Az	1.45	0.196	89.9	106.5	12.3	2.6	1.3	60.7
5% Az	1.45	0.195	82.1	101.2	10.9	2.2	1.0	51.0
10% Az	1.46	0.191	63.7	80.2	8.7	1.9	0.94	44.8
25% Az	1.47	0.187	31.3	52.3	4.7	1.0	0.50	23.6
50% Az	1.48	0.175	32.3	47.7	3.2	0.56	0.26	14.2
75% Az	1.49	0.172	24.3	36.1	2.0	0.36	0.15	8.6
90% Az	1.50	0.162	27.9	41.7	1.9	0.35	0.14	9.0
95% Az	1.50	0.159	23.6	44.1	1.7	0.30	0.13	8.4
100% Az	1.51	0.151	13.2	33.5	1.5	0.25	0.10	6.0
0% T	1.46	0.193	67.6	105.6	10.5	2.0	1.2	51.1
5% T	1.47	0.189	67.8	83.0	8.3	1.7	0.90	40.4
10% T	1.47	0.188	60.1	75.6	7.3	1.3	0.77	33.3
25% T	1.48	0.183	50.0	60.9	4.8	0.96	0.51	23.3
50% T	1.48	0.175	47.1	67.9	4.3	0.77	0.37	16.9
75% T	1.48	0.173	42.0	39.0	2.2	0.39	0.20	9.0
90% T	1.51	0.156	32.2	59.9	2.0	0.35	0.20	8.7
95% T	1.51	0.155	29.8	48.6	1.9	0.32	0.19	8.7
100% T	1.52	0.151	19.5	34.6	1.8	0.34	0.17	8.1
0% Ch	1.46	0.195	93.3	109.2	12.9	2.7	1.4	63.8
5% Ch	1.46	0.195	92.4	108.1	12.8	2.6	1.3	62.6
10% Ch	1.46	0.193	88.2	104.9	11.9	2.5	1.3	59.8
25% Ch	1.46	0.187	79.6	96.3	9.8	2.1	1.0	47.8
50% Ch	1.46	0.180	65.5	82.4	7.7	1.5	0.80	36.0
75% Ch	1.45	0.174	54.0	70.8	6.2	1.3	0.65	28.2
90% Ch	1.45	0.173	50.0	67.0	5.5	1.1	0.60	25.0
95% Ch	1.45	0.172	45.1	64.9	5.0	1.0	0.58	22.7
100% Ch	1.45	0.172	43.6	62.0	4.8	0.98	0.54	20.6

polymers. The first one is the Bondi approach of van der Waals volume (Vw) calculation by the group contribution method.⁵⁵ This approach is widely used and gives Vw values comparable to those that can be found in the literature only for the homopolymers, 44,56 since the copolymers studied in this work are synthesized for the first time. The second method uses a molecular modeling software, e.g., HyperChem or Material Studio, for calculations of the Vw of the monomeric unit in the macromolecular chain, by applying parameters obtained from a geometrically optimized polymer chain, that consists of at least 10 monomeric units. By this approach, the FFV values are much higher than by using the Bondi group contribution method approach. Computational methods are normally a good approach for the estimation of physical properties of polymers including polymer chain packing, 56,57 but to date the most accepted approach for FFV calculation of polymers that are relevant for gas separation is the use of the Bondi group contribution method. In terms of final value, the differences between both methods are evident, as it was as well reported in previous studies; 58 on the other hand, evolution of the FFV as a function of the polymer composition is similar for both computation methods. In this work, the Bondi group contribution method was employed in order to analyze the differences between the imidization methods and copolymer composition.

Density values for the polymers imidized by azeotropic and thermal methods are higher than those for the samples imidized by chemical imidization, and therefore the FFV for chemically imidized samples was higher compared to both other methods. This is in agreement with the determined density values. This

phenomenon can be explained by the different polymer intraand interchain interactions in Az- and T- compared to Chimidized polymers. Hydroxyl groups are capable of taking part in hydrogen bonding, increasing the intra- and interchain interactions and reducing the FFV. 59,60 The substitution of the hydroxyl groups by acetate groups reduces chain interactions, generating a larger FFV. Surprisingly, the homopolymers imidized by different methods derived from 6FDA-6FpDA showed slight differences in the FFV. Such differences were also found between the copolymers imidized by azeotropic and thermal methods, despite the fact that according to the ¹H NMR study the polymer structure was the same for all imidization methods. These small differences between theoretically similar polymers could be an indication of different polymer chain packing depending on the imidization method, which cannot be reflected in the van der Waals volume calculations. The FFV for thermally imidized polymers showed lower values than the azeotropic imidized, which could be an indication of additional interactions between polymer chains, as it can originate from for example cross-linking reactions occurring during imidization process, which were described elsewhere. 61 Thermally imidized polymers were completely soluble in regular solvents such as THF or DMSO, which contradicts the idea of cross-linking, but this is mainly due to the bulky hexafluoroisopropylidene moieties in dianhydride and diamine monomers whose presence clearly improves the solubility of the polyimides.

Table 2 summarizes the results of gas permeation experiments for all the studied samples. As it was expected, changes of the permeability coefficients were consistent with the changes

in the FFV of studied polymers. Unexpected was the variation of the permeability values for the homopolymers derived from 6FDA-6FpDA imidized by different methods, despite their exactly identical chemical structure. It reveals that the polymer chain packing depends strongly on the imidization method supporting the idea that imidization methods influence the interchain interactions. The described effect was also evident when small amounts of the second comonomer, such as 5–10 mol %, were copolymerized. This evolution can be easily followed in Figure 8.

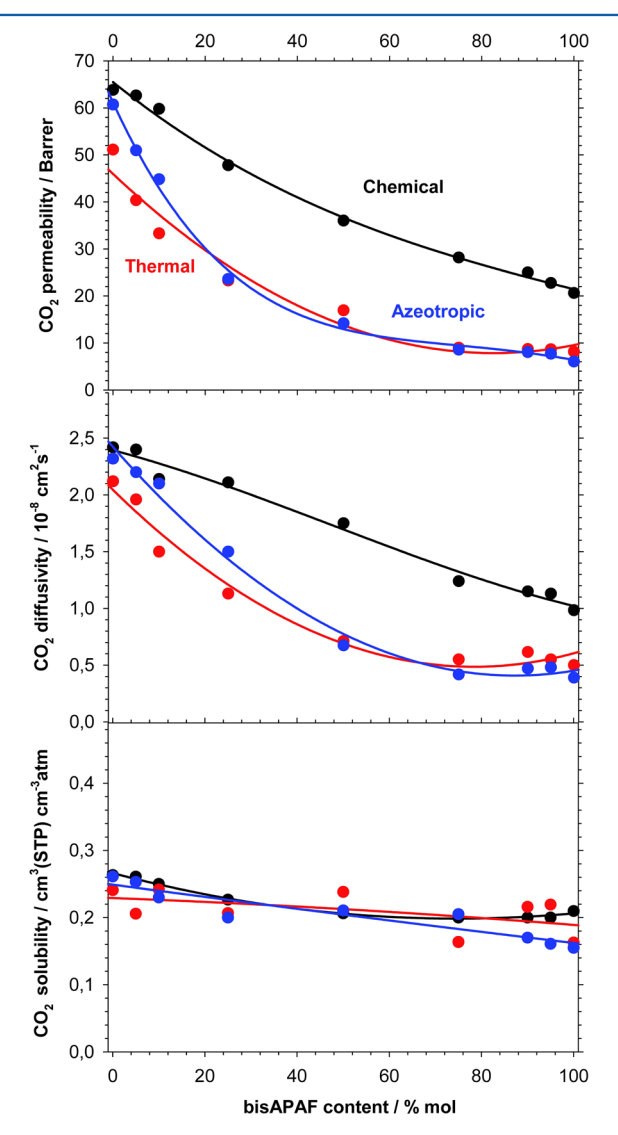


Figure 8. Evolution of CO_2 permeability, diffusivity, and solubility as a function of composition and imidization method.

In general, for all imidization methods employed in this work, the 100 mol % bisAPAF content samples presented permeability values in the same order than in previous works, ^{59,62} and these permeabilities were much lower than for polymers without bisAPAF. Therefore, the copolymers showed a clear evolution between those two polymer compositions. In the case of the chemically imidized samples, the permeability decrease was almost linearly dependent on the bisAPAF content. For the azeotropically and thermally imidized samples a more complex dependence was observed. The permeability coefficients for bisAPAF contents up to 50 mol % show an

inverse relationship with respect to the percentage of the bisAPAF content. Therefore, a rapid decrease of the permeability coefficients is observed, followed by reaching a constant level for the permeability coefficients for higher bisAPAF contents. The differences in the permeability results for samples derived from 6FDA-BisAPAF revealed the effect of having acetate groups instead of hydroxyl group in the structure, leading to more than 2-fold higher permeability values for the acetylated samples. It can be expected that the copolymer permeabilities follow a nearly linear dependence on the content of the homopolymers, as in the case of the chemically imidized polymers, as it would be expected from the Maxwell model.⁶³ This is definitely not the case for thermally and azeotropically imidized samples. This is most probably due to the presence of some additional factors, such as polymer interchain interactions.

From the analysis of the CO₂ permeability for samples imidized by azeotropic and thermal methods, two different areas can be distinguished (Figure 8). At low bisAPAF contents, between 0 and 10 mol %, significant differences in the properties of the polymers that were imidized by these two methods originating probably from chain packing effect can be observed. Moreover, the existence of secondary reactions, such as cross-linking reactions, which occur during the thermal imidization, promotes the observed change in material properties. 64-66 For the rest of the bisAPAF contents, in the range of 25–100 mol %, both polymer types showed practically the same behavior. The reason could be associated with having a larger amount of the second monomer (bisAPAF) in the structure, which favors the interchain interactions and reduces the polymer chain mobility. This fact could be compared with the typical percolation behavior in copolymers, in which surpassing a certain percentage of one comonomer in the copolymer composition restricts the properties of the predominant material.⁶⁷ For chemically imidized samples, the elimination of the hydrogen bond interactions resulted in higher permeabilities compared to the other two imidization methods.⁶² Even for low percentages, it is possible to see a big effect on the permeability as a result of higher diffusivity values. Independently of the imidization method, solubility values decrease almost linearly with the percentage of bisAPAF, indicating the higher solubility factor of the monomer 6FpDA. The structure is the same for samples obtained by azeotropic and thermal imidization and very similar for chemically imidized samples. From these facts we concluded that the presence of acetate groups compared to hydroxyl groups gives a small variation in the CO₂ solubility. For the diffusivity, the effect of the acetate group is more intense. The incorporation of this group in the structure eliminates the interchain interaction due to hydrogen bonds, leading to an increase in the diffusivity compared to the structures with unmodified hydroxyl groups.

For chemically imidized polymers, the $\rm CO_2/CH_4$ selectivity was constant for bisAPAF contents between 0 and 50%, as it can be observed in Figure 9. After that point, the selectivity decreases from 45 to 38. The reduction of the selectivity for chemically imidized samples for bisAPAF contents higher than 50 mol % clearly correlates with the reduction of the diffusivity selectivity, since the reduction in the polymer chain packing ability leads to a less selective material. Unexpected differences between azeotropic and thermal imidized polymers were observed in the tendency of the $\rm CO_2/CH_4$ selectivity values. For both sets of polymers, the selectivity is increasing when the

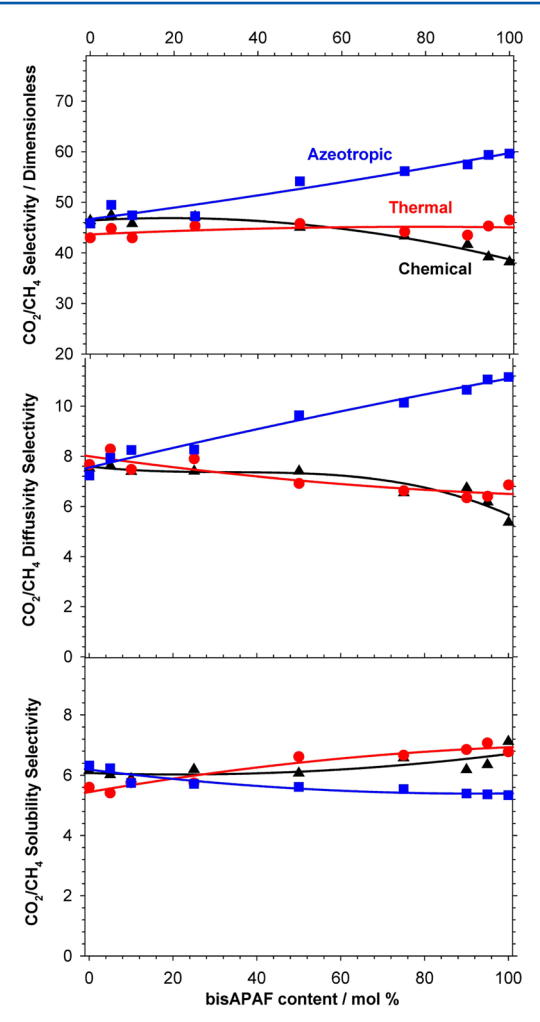


Figure 9. Evolution of permeability, diffusivity, and solubility selectivity as a function of polyimide composition and imidization method for the CO_2/CH_4 gas pair.

amount of bisAPAF in the polymer is increasing. This observation is attributed to the presence of hydrogen bonds which reduces the interchain space. For thermally imidized polymers the selectivity increased from 43 to 46, while azeotropically imidized polymers showed an increase from 46 to 59. In order to understand the reasons of this atypical behavior, the gas transport parameters influencing the permeability and thus permeability selectivity, i.e., diffusivity selectivity (α_D) and solubility selectivity (α_S) , were also analyzed. For the thermally imidized samples a slight selectivity increase was observed, which can be related mainly to the increase in the solubility selectivity, as is depicted in Figure 8. Possible cross-linking reactions during the imidization process can result in reduced α_D but increased α_S , which, in this case, is the predominant factor. Surprisingly, for the azeotropically imidized samples an almost linear increase of the CO₂/CH₄ selectivity was observed. Solubility selectivity α_S for these sets of samples was almost constant, but $\alpha_{\rm D}$ was linearly augmented when the amount of the hydrogen-bond-forming monomer bisAPAF is increased. Higher freedom in the mobility of the polymer chains in the case of Az samples compared to T samples leads to the possibility of a better polymer chain packing, increasing the diffusivity selectivity parameter and therefore the overall selectivity for CO₂/CH₄ pair of gases.

Similar tendencies were observed for other pair of gases as Figure 10 shows for O_2/N_2 and CO_2/N_2 .

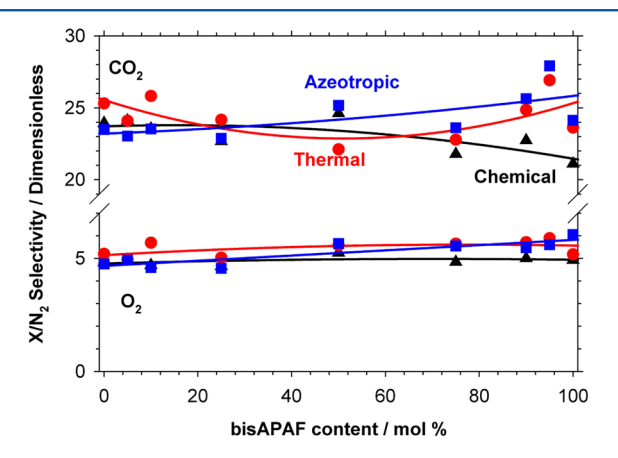


Figure 10. Evolution of permeability selectivity as a function of composition and imidization method for the $\rm O_2/N_2$ and $\rm CO_2/N_2$ gas pairs.

Table 3 shows the results for several gas pairs. It is clear again that an increase in the hydroxyl groups in the polymer leads to

Table 3. Ideal Selectivities for Several Gas Pairs (30 $^{\circ}$ C and Feed Pressure 1000 mbar)

	selectivity (dimensionless)					
sample	CO ₂ /CH ₄	H ₂ /CH ₄	O_2/N_2	CO ₂ /N ₂		
0% Az	46.7	69.2	4.7	23.3		
5% Az	51.0	82.1	5.0	23.2		
10% Az	47.7	67.8	4.6	23.6		
25% Az	47.2	62.6	4.7	23.6		
50% Az	54.6	124.2	5.7	25.4		
75% Az	57.3	162.0	5.6	23.9		
90% Az	64.3	199.3	5.4	25.7		
95% Az	64.6	181.5	5.7	28.0		
100% Az	60.0	132.0	6.0	24.0		
0% T	42.6	56.3	5.3	25.6		
5% T	44.9	75.3	4.9	23.8		
10% T	43.2	78.1	5.6	25.6		
25% T	45.7	98.0	5.0	24.3		
50% T	45.7	127.3	5.6	21.9		
75% T	45.0	210.0	5.6	23.1		
90% T	43.5	161.0	5.7	24.9		
95% T	45.8	156.8	5.9	27.2		
100% T	47.6	114.7	5.3	23.8		
0% Ch	45.6	66.6	4.8	23.6		
5% Ch	48.2	71.1	4.9	24.1		
10% Ch	46.0	67.8	4.8	23.9		
25% Ch	47.8	79.6	4.7	22.8		
50% Ch	45.0	81.9	5.1	24.0		
75% Ch	43.4	83.1	4.8	21.7		
90% Ch	41.7	83.3	5.0	22.7		
95% Ch	39.1	77.8	5.0	22.7		
100% Ch	38.1	80.7	4.9	21.0		

an increase of the $\alpha_{\rm D}$ as it was mentioned before. This is even clearer for the gas pair ${\rm H_2/CH_4}$ where due to the different in size, the $\alpha_{\rm D}$ is clearly predominant. The comparison between chemically, azeotropically, and thermally imidized polymers shows the importance of the existence of hydroxyl groups in the

structure as it was concluded in previous works.^{59,60} It is interesting to notice that the selectivity increased rapidly for copolymers with more than 50 mol % content of bisAPAF, indicating that at that point the number of hydroxyl groups in the copolymer is controlling the separation mechanism.

The influence of the interchain interactions due to hydrogen bond formation can be analyzed in terms of the hydroxyl group content in the polymers. The mol % content of hydroxyl groups in the different structures can be calculated according to the following equation:

mol % OH groups

$$= \frac{\left(\frac{2 \times \text{molar mass OH} \times 100}{\text{molar mass bisAPAF}}\right) \times \text{bisAPAF content (\%)}}{\text{molar mass of the copolymer}}$$
(6)

In this sense, Figure 11 shows the evolution of the CO_2 permeability as a function of the -OH content in the polymer.

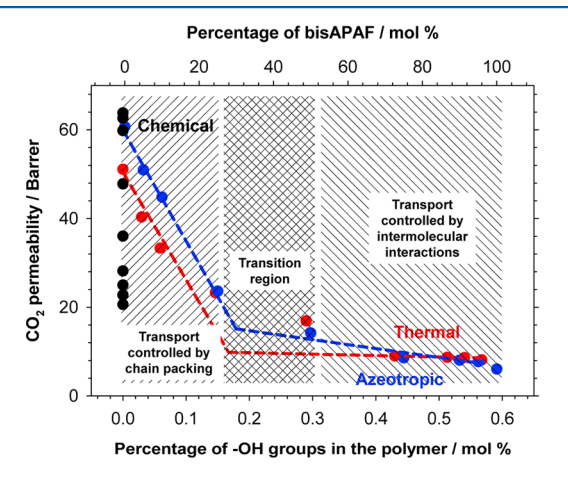


Figure 11. CO₂ permeability as a function of the percentage of hydroxyl group in the copolymer.

Three different regions can be expected according to the effective medium theory. ^{67,68} In the first region, for low content of hydroxyl groups in the polymer, lower than 30 mol % of BisAPAF in the polymer, the influence of the polymer chain packing ability is predominant in the transport mechanism. For high content of hydroxyl groups in the polymer, higher than 50 mol % of BisAPAF in the polymer, the gas transport mechanism is controlled by the intermolecular interactions caused by hydrogen bonds. Between these two regions, there is an area where the effect is a combination of both situations, a "transition region". By means of a line fitting analysis of the marginal situations of either low or high contents of the bisAPAF comonomer in the final structure, it is possible to identify the bisAPAF content in the polyimides at which the hydrogen bond interactions between different polymer chains start to become predominant in the transport mechanism.

The chemically imidized polymers are not included in the discussion due to the zero or very low hydroxyl group content; that is leading to a transport mechanism, which is obviously controlled by the polymer chain packing ability. Despite the fact that thermal and azeotropic imidization methods showed similar tendencies, small differences can be still observed. Because of the secondary cross-linking reactions, the thermally imidized polymers need a lower content of hydroxyl groups than azeotropically imidized polymers to have a transport mechanism that is controlled by intermolecular interactions.

These crossing lines correspond to bisAPAF contents of around 30 mol % for these imidization methods. Once the predominant effect is the hydrogen bonding, the differences between both imidization methods, thermal and azeotropic, are minimal.

CONCLUSIONS

A set of 27 polyimides comprised of nine different composition groups, which were imidized by three methods—azeotropic, thermal, and chemical—were prepared. Two different fluorinated diamines, 6FpDA (x) and bisAPAF (y), which have a hydroxyl *ortho*-functional group to the amine, and one fluorinated dianhydride, 6FDA, were employed in different amounts (where y = 0, 5, 10, 25, 50, 75, 90, 95, and 100 mol %).

For the 6FDA-6FpDA homopolymers, where y=0, regardless of the imidization method, the resulting polymer structure is the same. Small differences in glass transition temperatures density values (thermal \geq chemical > azeotropic) were identified, which is an indication of the existence of small differences in the interchain interactions between the polymer chains. During the evaluation of the data on CO_2/CH_4 gas pair separation, it was found that more significant differences between properties of polymers imidized by different methods (chemical \geq azeotropic > thermal) were found. This was mainly attributed to the diffusivity factor, which is an indication of the influence of the imidization method in the polymer chains' packing.

By introduction of the BisAPAF in the polymer, for thermally and azeotropically imidized samples, hydroxyl-containing moieties are present in the polyimide structure, while for chemically imidized samples acetate groups' presence in the resulting polymer was confirmed. The substitution of hydroxyl groups by acetate groups leads to a completely different chain packing and therefore different properties of the materials. At higher amounts of bisAPAF, differences between chemical and the two imidization routes are more evident. In chemically imidized samples, the possibility of hydrogen bond formation is eliminated by esterification with acetic anhydride, leading to lower T_g values, higher FFV, and higher values of permeability for all the gases tested, compared to azeotropically and thermally imidized samples. Theoretically, the same polymer structures are obtained by azeotropic and thermal imidizations, but subtle differences in the properties were still found. For thermally treated samples, higher T_g , lower FFV, and lower permeability values were found, which were especially evident for low values of bisAPAF content, indicating that the thermally imidized homopolymer 6FDA-6FpDA could be more predisposed to the cross-linking reactions. Surprisingly, statistically relevant differences in the selectivity factors were found between those two imidization methods mainly due to the diffusivity selectivity, which definitely indicates that the imidization method affects the packing way of the polymer

Tendencies are clearly explained by analysis of the interchain interactions arising from the hydroxyl groups' presence in the studied polymers. Depending on the hydroxyl group content, three different areas were identified. The gas transport mechanism is mainly controlled by the chain packing for thermally and azeotropically imidized polymers with bisAPAF contents lower than 30 mol %. At high bisAPAF content, above 50 mol %, the gas transport is controlled by the intermolecular

1

interactions, such as hydrogen bonds. Between these two areas, the transport mechanism is a combination of both situations.

AUTHOR INFORMATION

Corresponding Author

*E-mail alberto.tena@hzg.de (A.T.).

ORCID

Alberto Tena: 0000-0001-9078-3990 Volker Abetz: 0000-0002-4840-6611

Notes

The authors declare no competing financial interest.

ACKNOWLEDGMENTS

This work was financially supported by Helmholtz Zentrum Geesthacht (HZG) through the technology transfer project program and by the Helmholtz Association of German Research Centers through the Helmholtz Portfolio MEMBRAIN. The authors thank S. Neumann and M. Brinkmann for technical support and Dr. S. Rangou and Dr. M. de la Viuda for scientific discussions.

REFERENCES

- (1) Fink, J. K. High Performance Polymers; William Andrew: 2014.
- (2) Handa, N. V.; Li, S.; Gerbec, J. A.; Sumitani, N.; Hawker, C. J.; Klinger, D. Fully Aromatic High Performance Thermoset via Sydnone–Alkyne Cycloaddition. *J. Am. Chem. Soc.* **2016**, *138*, 6400.
- (3) Bacosca, I.; Hamciuc, E.; Bruma, M.; Ignat, M. Poly(amide imide)s containing functional nitrile groups for high performance materials. *React. Funct. Polym.* **2011**, *71* (8), 905–915.
- (4) Liaw, D.-J.; Wang, K.-L.; Huang, Y.-C.; Lee, K.-R.; Lai, J.-Y.; Ha, C.-S. Advanced polyimide materials: syntheses, physical properties and applications. *Prog. Polym. Sci.* **2012**, *37* (7), 907–974.
- (5) Huda, Z.; Edi, P. Materials selection in design of structures and engines of supersonic aircrafts: a review. *Mater. Eng.* **2013**, *46*, 552–560.
- (6) Damaceanu, M.-D.; Constantin, C.-P.; Nicolescu, A.; Bruma, M.; Belomoina, N.; Begunov, R. S. Highly transparent and hydrophobic fluorinated polyimide films with ortho-kink structure. *Eur. Polym. J.* **2014**, *50*, 200–213.
- (7) Sroog, C. E. Polyimides. Macromol. Rev. 1976, 11 (1), 161–208.
- (8) Bessonov, M. I.; Zubkov, V. A. Polyamic Acids and Polyimides: Synthesis, Transformations, and Structure; Taylor & Francis: 1993.
- (9) Okamoto, K.-i.; Fuji, M.; Okamyo, S.; Suzuki, H.; Tanaka, K.; Kita, H. Gas permeation properties of poly(ether imide) segmented copolymers. *Macromolecules* **1995**, 28 (20), 6950–6956.
- (10) Furusho, Y.; Ito, Y.; Kihara, N.; Osakada, K.; Suginome, M.; Takata, T.; Takeuchi, D. *Polymer Synthesis*; Springer: Berlin, 2004.
- (11) Tena, A.; Marcos-Fernandez, A.; Lozano, A.; de Abajo, J.; Palacio, L.; Prádanos, P.; Hernández, A. Influence of the PEO length in gas separation properties of segregating aromatic—aliphatic copoly (ether-imide) s. *Chem. Eng. Sci.* 2013, 104, 574—585.
- (12) Coletta, E.; Toney, M. F.; Frank, C. W. Influences of liquid electrolyte and polyimide identity on the structure and conductivity of polyimide—poly (ethylene glycol) materials. *J. Appl. Polym. Sci.* **2015**, 132 (12), 41675.
- (13) Hernández, G.; Casado, N.; Coste, R.; Shanmukaraj, D.; Rubatat, L.; Armand, M.; Mecerreyes, D. Redox-active polyimide—polyether block copolymers as electrode materials for lithium batteries. *RSC Adv.* **2015**, *5* (22), 17096–17103.
- (14) Tena, A.; Marcos-Fernández, Á.; de la Viuda, M.; Palacio, L.; Prádanos, P.; Lozano, Á. E.; de Abajo, J.; Hernández, A. Advances in the design of co-poly(ether-imide) membranes for CO₂ separations. Influence of aromatic rigidity on crystallinity, phase segregation and gas transport. *Eur. Polym. J.* **2015**, *62*, 130–138.

(15) Kim, W. G.; Hay, A. S. Synthesis of soluble poly(ether imides) from bis(ether anhydrides) containing bulky substituents. *Macromolecules* **1993**, 26 (20), 5275–5280.

- (16) Kusama, M.; Matsumoto, T.; Kurosaki, T. Soluble Polyimides with Polyalicyclic Structure.3. Polyimides from (4arH,8acH)-Decahydro-1t,4t:5c,8c-dimethanonaphthalene- 2t,3t,6c,7c-tetracarboxylic 2,3:6,7-Dianhydride. *Macromolecules* 1994, 27 (5), 1117–1123.
- (17) Chen, J. P.; Natansohn, A. Synthesis and Characterization of Novel Carbazole-Containing Soluble Polyimides. *Macromolecules* **1999**, 32 (10), 3171–3177.
- (18) Matsumoto, T. Nonaromatic Polyimides Derived from Cycloaliphatic Monomers. *Macromolecules* **1999**, 32 (15), 4933–4939.
- (19) Grazulevicius, J. V.; Strohriegl, P.; Pielichowski, J.; Pielichowski, K. Carbazole-containing polymers: synthesis, properties and applications. *Prog. Polym. Sci.* **2003**, 28 (9), 1297–1353.
- (20) Liaw, D.-J.; Chang, F.-C.; Leung, M.-k.; Chou, M.-Y.; Muellen, K. High Thermal Stability and Rigid Rod of Novel Organosoluble Polyimides and Polyamides Based on Bulky and Noncoplanar Naphthalene—Biphenyldiamine. *Macromolecules* **2005**, 38 (9), 4024—4029.
- (21) Butt, M. S.; Akhter, Z.; zafar Zaman, M. Synthesis and Characterization of Polyimides Based on Flexible Diamine. *Eur. Chem. Bull.* **2013**, 2 (9), 631–636.
- (22) Banerjee, S. Handbook of Specialty Fluorinated Polymers: Preparation, Properties, and Applications; Elsevier Science: 2015.
- (23) Damaceanu, M. D.; Rusu, R. D.; Musteata, V. E.; Bruma, M. Insulating polyimide films containing n-type perylenediimide moieties. *Polym. Int.* **2012**, *61* (10), 1582–1591.
- (24) Jia, M.; Li, Y.; He, C.; Huang, X. Soluble Perfluorocyclobutyl Aryl Ether-Based Polyimide for High-Performance Dielectric Material. *ACS Appl. Mater. Interfaces* **2016**, *8* (39), 26352–26358.
- (25) Bruma, M.; Fitch, J. W.; Cassidy, P. E. Hexafluoroisopropylidene-Containing Polymers for High-Performance Applications. *J. Macromol. Sci., Polym. Rev.* **1996**, 36 (1), 119–159.
- (26) Lim, H.; Cho, W. J.; Ha, C. S.; Ando, S.; Kim, Y. K.; Park, C. H.; Lee, K. Flexible Organic Electroluminescent Devices Based on Fluorine-Containing Colorless Polyimide Substrates. *Adv. Mater.* **2002**, *14* (18), 1275–1279.
- (27) Damaceanu, M.-D.; Rusu, R.-D.; Bruma, M.; Rusanov, A. L. New thermally stable and organosoluble heterocyclic poly-(naphthaleneimide)s. *Polym. Adv. Technol.* **2011**, 22 (4), 420–429.
- (28) Wang, Y.-C.; Huang, S.-H.; Hu, C.-C.; Li, C.-L.; Lee, K.-R.; Liaw, D.-J.; Lai, J.-Y. Sorption and transport properties of gases in aromatic polyimide membranes. *J. Membr. Sci.* **2005**, 248 (1–2), 15–25
- (29) Calle, M.; Lozano, A. E.; de Abajo, J.; de la Campa, J. G.; Álvarez, C. Design of gas separation membranes derived of rigid aromatic polyimides. 1. Polymers from diamines containing di-tert-butyl side groups. *J. Membr. Sci.* **2010**, 365 (1–2), 145–153.
- (30) Park, J. Y.; Paul, D. R. Correlation and prediction of gas permeability in glassy polymer membrane materials via a modified free volume based group contribution method. *J. Membr. Sci.* **1997**, *125* (1), 23–39.
- (31) Tanaka, K.; Kita, H.; Okano, M.; Okamoto, K.-i. Permeability and permselectivity of gases in fluorinated and non-fluorinated polyimides. *Polymer* **1992**, 33 (3), 585–592.
- (32) Hougham, G.; Tesoro, G.; Shaw, J. Synthesis and Properties of Highly Fluorinated Polyimides. *Macromolecules* **1994**, 27 (13), 3642–3649.
- (33) Coleman, M. R.; Koros, W. J. Isomeric polyimides based on fluorinated dianhydrides and diamines for gas separation applications. *J. Membr. Sci.* **1990**, *50* (3), 285–297.
- (34) Ghosh, M. Polyimides: Fundamentals and Applications; Taylor & Francis: 1996.
- (35) Joly, C.; Le Cerf, D.; Chappey, C.; Langevin, D.; Muller, G. Residual solvent effect on the permeation properties of fluorinated polyimide films. *Sep. Purif. Technol.* **1999**, *16* (1), 47–54.
- (36) Wind, J. D.; Staudt-Bickel, C.; Paul, D. R.; Koros, W. J. The Effects of Crosslinking Chemistry on CO₂ Plasticization of Polyimide

Gas Separation Membranes. Ind. Eng. Chem. Res. 2002, 41 (24), 6139-6148.

- (37) Merkel, T. C.; Pinnau, I.; Prabhakar, R.; Freeman, B. D., Gas and Vapor Transport Properties of Perfluoropolymers. In *Materials Science of Membranes for Gas and Vapor Separation*; John Wiley & Sons, Ltd.: 2006; pp 251–270.
- (38) Recio, R.; Palacio, L.; Prádanos, P.; Hernández, A.; Lozano, Á. E.; Marcos, Á.; de la Campa, J. G.; de Abajo, J. Gas separation of 6FDA–6FpDA membranes: Effect of the solvent on polymer surfaces and permselectivity. *J. Membr. Sci.* **2007**, 293 (1–2), 22–28.
- (39) Munoz, D. M.; Calle, M.; de La Campa, J. G.; de Abajo, J.; Lozano, A. E. An improved method for preparing very high molecular weight polyimides. *Macromolecules* **2009**, 42 (15), 5892–5894.
- (40) Kratochvil, A. M.; Koros, W. J. Effects of Supercritical CO₂ Conditioning on Cross-Linked Polyimide Membranes. *Macromolecules* **2010**, 43 (10), 4679–4687.
- (41) Tena, A.; Fernández, L.; Sánchez, M.; Palacio, L.; Lozano, A. E.; Hernández, A.; Prádanos, P. Mixed matrix membranes of 6FDA-6FpDA with surface functionalized γ -alumina particles. An analysis of the improvement of permselectivity for several gas pairs. *Chem. Eng. Sci.* **2010**, 65 (6), 2227–2235.
- (42) Neyertz, S.; Brown, D. The effect of structural isomerism on carbon dioxide sorption and plasticization at the interface of a glassy polymer membrane. *J. Membr. Sci.* **2014**, *460*, 213–228.
- (43) Plaza-Lozano, D.; Comesaña-Gándara, B.; de la Viuda, M.; Seong, J. G.; Palacio, L.; Prádanos, P.; de la Campa, J. G.; Cuadrado, P.; Lee, Y. M.; Hernández, A.; Alvarez, C.; Lozano, A. E. New aromatic polyamides and polyimides having an adamantane bulky group. *Materials Today Communications* **2015**, *5*, 23–31.
- (44) Han, S. H.; Misdan, N.; Kim, S.; Doherty, C. M.; Hill, A. J.; Lee, Y. M. Thermally Rearranged (TR) Polybenzoxazole: Effects of Diverse Imidization Routes on Physical Properties and Gas Transport Behaviors. *Macromolecules* **2010**, *43* (18), 7657–7667.
- (45) Park, H. B.; Jung, C. H.; Lee, Y. M.; Hill, A. J.; Pas, S. J.; Mudie, S. T.; Van Wagner, E.; Freeman, B. D.; Cookson, D. J. Polymers with Cavities Tuned for Fast Selective Transport of Small Molecules and Ions. *Science* **2007**, *318* (5848), 254–258.
- (46) Tena, A.; Rangou, S.; Shishatskiy, S.; Filiz, V.; Abetz, V. Claisen thermally rearranged (CTR) polymers. *Sci. Adv.* **2016**, 2 (7), e1501859.
- (47) Pye, D. G.; Hoehn, H. H.; Panar, M. Measurement of gas permeability of polymers. I. Permeabilities in constant volume/variable pressure apparatus. *J. Appl. Polym. Sci.* **1976**, 20 (7), 1921–1931.
- (48) Shishatskii, A. M.; Yampol'skii, Y. P.; Peinemann, K. V. Effects of film thickness on density and gas permeation parameters of glassy polymers. *J. Membr. Sci.* 1996, 112 (2), 275–285.
- (49) Tena, A.; Marcos-Fernández, A.; Lozano, A. E.; de la Campa, J. G.; de Abajo, J.; Palacio, L.; Prádanos, P.; Hernández, A. Thermally treated copoly(ether-imide)s made from bpda and alifatic plus aromatic diamines. Gas separation properties with different aromatic diamimes. J. Membr. Sci. 2012, 387–388, 54–65.
- (50) Windrich, F.; Kappert, E. J.; Malanin, M.; Eichhorn, K.-J.; Häu β ler, L.; Benes, N. E.; Voit, B. In-situ imidization analysis in microscale thin films of an ester-type photosensitive polyimide for microelectronic packaging applications. *Eur. Polym. J.* **2016**, *84*, 279–291.
- (51) Swaidan, R. J.; Ma, X.; Litwiller, E.; Pinnau, I. Enhanced propylene/propane separation by thermal annealing of an intrinsically microporous hydroxyl-functionalized polyimide membrane. *J. Membr. Sci.* **2015**, *495*, 235–241.
- (52) Kotov, B. V.; Gordina, T. A.; Voishchev, V. S.; Kolninov, O. V.; Pravednikov, A. N. Aromatic polyimides as charge transfer complexes. *Polym. Sci. U. S. S. R.* **1977**, *19* (3), 711–716.
- (53) Likhatchev, D.; Gutierrez-Wing, C.; Kardash, I.; Vera-Graziano, R. Soluble aromatic polyimides based on 2,2-bis(3-amino-4-hydroxyphenyl)hexafluoropropane: Synthesis and properties. *J. Appl. Polym. Sci.* **1996**, 59 (4), 725–735.
- (54) Banerjee, S.; Madhra, M. K.; Salunke, A. K.; Maier, G. Synthesis and properties of fluorinated polyimides. 1. Derived from novel 4, 4

- "-bis (aminophenoxy)-3, 3 "-trifluoromethyl terphenyl. J. Polym. Sci., Part A: Polym. Chem. 2002, 40 (8), 1016–1027.
- (55) Bondi, A. van der Waals Volumes and Radii. J. Phys. Chem. 1964, 68 (3), 441–451.
- (56) Wang, X.-Y.; in 't Veld, P. J.; Lu, Y.; Freeman, B. D.; Sanchez, I. C. A molecular simulation study of cavity size distributions and diffusion in para and meta isomers. *Polymer* **2005**, *46* (21), 9155–9161.
- (57) Thran, A.; Kroll, G.; Faupel, F. Correlation between fractional free volume and diffusivity of gas molecules in glassy polymers. *J. Polym. Sci., Part B: Polym. Phys.* **1999**, *37* (23), 3344–3358.
- (58) Heuchel, M.; Hofmann, D.; Pullumbi, P. Molecular Modeling of Small-Molecule Permeation in Polyimides and Its Correlation to Free-Volume Distributions. *Macromolecules* **2004**, *37* (1), 201–214.
- (59) Jung, C. H.; Lee, Y. M. Gas permeation properties of hydroxylgroup containing polyimide membranes. *Macromol. Res.* **2008**, *16* (6), 555–560.
- (60) Alaslai, N.; Ghanem, B.; Alghunaimi, F.; Litwiller, E.; Pinnau, I. Pure- and mixed-gas permeation properties of highly selective and plasticization resistant hydroxyl-diamine-based 6FDA polyimides for CO₂/CH₄ separation. *J. Membr. Sci.* **2016**, 505, 100–107.
- (61) Calle, M.; Lozano, A. E.; Lee, Y. M. Formation of thermally rearranged (TR) polybenzoxazoles: Effect of synthesis routes and polymer form. *Eur. Polym. J.* **2012**, *48* (7), 1313–1322.
- (62) Swaidan, R.; Ghanem, B.; Litwiller, E.; Pinnau, I. Effects of hydroxyl-functionalization and sub-Tg thermal annealing on high pressure pure- and mixed-gas CO₂/CH4 separation by polyimide membranes based on 6FDA and triptycene-containing dianhydrides. *J. Membr. Sci.* **2015**, 475, 571–581.
- (63) Kerkhof, P. J. A. M. A modified Maxwell-Stefan model for transport through inert membranes: the binary friction model. *Chemical Engineering Journal and the Biochemical Engineering Journal* 1996, 64 (3), 319–343.
- (64) Kuroda, S.-i.; Mita, I. Degradation of aromatic polymers—II. The crosslinking during thermal and thermo-oxidative degradation of a polyimide. *Eur. Polym. J.* **1989**, *25* (6), 611–620.
- (65) Bos, A.; Pünt, I. G. M.; Wessling, M.; Strathmann, H. Plasticization-resistant glassy polyimide membranes for CO₂/CO4 separations. *Sep. Purif. Technol.* **1998**, *14* (1), 27–39.
- (66) Snyder, R. W.; Thomson, B.; Bartges, B.; Czerniawski, D.; Painter, P. C. FTIR studies of polyimides: thermal curing. *Macromolecules* **1989**, 22 (11), 4166–4172.
- (67) Tena, A.; de la Viuda, M.; Palacio, L.; Prádanos, P.; Marcos-Fernández, Á.; Lozano, Á. E.; Hernández, A. Prediction of gas permeability of block-segregated polymeric membranes by an effective medium model. *J. Membr. Sci.* **2014**, *453*, 27–35.
- (68) Landauer, R. The electrical resistance of binary metallic mixtures. J. Appl. Phys. 1952, 23 (7), 779–784.